JOURNAL OF MATERIALS SCIENCE 18 (1983) 864–883

Computer simulation of polyethylene crystals

Part 2 *The boundary properties of twins and stacking faults*

N. A. GEARY*, D. J. BACON
Department of Metallurgy and Materials Science, The University of Liverpool, P.O. Box 147, Liverpool, UK

The computer programs described in Part 1 [9] have been used to investigate the structure and energy of stacking-faults and coherent twin boundaries in model polyethylene crystals. They are particularly relevant to the deformation behaviour of polyethylene, and it is explained how simulation studies can supplement experimental observations. Generalized translation faults have been simulated on the low-index planes of orthorhombic and monoclinic crystals constructed from rigid molecular chains of infinite length, and the stable faults have been identified. In the former structure, the only faults of significance are on the {1 1 0} planes, and three different configurations exist, each of energy $\sim 10\,mJ\,m^{-2}$. In the monoclinic phase, two stable faults occur on each of the planes (1 0 0) and (0 1 0), and in both cases the most stable fault has an energy $\sim 3\,mJ\,m^{-2}$. The possible implications of these findings for chain-axis and transverse slip in the two crystal structures are discussed. The structures of the coherent boundaries of {1 1 0} and {3 1 0} twins in orthorhombic and (1 0 0) and (0 1 0) twins in monoclinic crystals have been investigated, and in all cases several stable configurations are possible. The {3 1 0} interfaces have high energy ($\gtrsim 30\,mJ\,m^{-2}$), whereas the others are similar in energy to the stacking faults. The results indicate the need to simulate incoherent boundaries. All the stable structures observed are found to have a simple geometrical explanation, and are not sensitive to the interatomic potentials used.

1. Introduction

The plastic behaviour under load of polymer crystals, and consequently of semicrystalline polymers, is dependent upon their ability to deform by shear in a variety of modes. As discussed in several reviews [1–3], they exhibit dislocation slip, twinning and martensitic transformations, these mechanisms having been most widely studied in polyethylene of orthorhombic crystal structure.

The slip systems reported do not break the molecules, and so the slip planes are all of the [0 0 1] zone. The two basic forms of slip must involve shears either parallel or perpendicular to [0 0 1], the chain axis, and the planes and directions of the slip systems are therefore either $(hk0)$ [0 0 1] or $(hk0)$ $[k\bar{h}0]$, respectively. The former "chain-axis" slip system is believed to result from the movement of [0 0 1] screw dislocations, for which good evidence exists [3]. The latter "transverse" system can take various forms, in principle, owing to the variety of possible Burgers vectors. The shortest lattice vector is [0 1 0], and the (1 0 0) [0 1 0] system is, therefore, anticipated on dislocation-energy grounds to be preferred to (0 1 0) [1 0 0], which involves the next shortest vector. Whilst length of Burgers vector might appear to rule out the third system, $\{1\bar{1}0\}\langle 1\,1\,0\rangle$, it was suggested by Frank *et al.* [4] that the perfect dislocation involved may dissociate into two partials by a reaction of the form

$$\langle 1\,1\,0\rangle \rightarrow \tfrac{1}{2}\langle 1\,1\,\epsilon\rangle + \tfrac{1}{2}\langle 1\,1\,\bar{\epsilon}\rangle. \qquad (1)$$

If ϵ is small, each partial vector can have a length shorter than [0 1 0]: it must be emphasized, how-

*Present address: EPS Consultants Ltd., Boundary House, Boston Road, London, W7 2QE, UK.

0022–2461/83/030864–20$04.90/0

ever, that this dissociation requires a stable stacking fault on $\{1\bar{1}0\}$. Although its existence has been inferred by Holland [5] with the observation of terminating $\{1\bar{1}0\}$ fold planes in overlapping crystal lamellae, there is no information about the energy, translation vector and structure of the fault. (Nor is it certain that faults cannot exist on other planes.) This is unfortunate as far as the theoretical description of deformation mechanisms is concerned, for slip competes with twinning under some loadings.

Twinning involving shear perpendicular to [001] makes an important contribution to the plasticity of polyethylene. The first systematic study of twinning as a contribution to deformation was by Frank *et al.* [4], who concluded that twinning on $\{110\}$ and $\{310\}$ is most likely to occur in practice. The crystallographic elements of these twins are, in conventional notation [1],

$$K_1: (1\bar{1}0); K_2: (310); \eta_1: [110]; \eta_2: [1\bar{3}0]. \quad (2)$$

The magnitude of shear associated with these modes is 0.32, and plane-of-shear sketches for them are reproduced in Fig. 1a. Bevis and Crellin [6] analysed all the possible twin modes by treating every chain as a point in a two-dimensional lattice, and found that these modes have by far the lowest shear magnitude. Despite their reciprocal relationship, however, only $\{110\}$ twinning is usually observed in bulk oriented and single-crystal specimens [1–3]. $\{310\}$ twinning has been reported, as reviewed by Preedy and Wheeler [7], but it is not clear to what extent its occurence is dictated by surface folds and modes of stress. In the light of this preference, information on the molecular structure and energy of the boundary

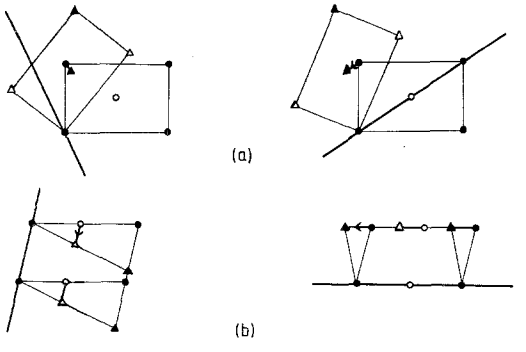

Figure 1 Plane-of-shear plots for (a) $(3\,1\,0)_0$ and $(\bar{1}\,1\,0)_0$ and (b) $(1\,0\,0)_m$ and $(0\,1\,0)_m$ twinning. Molecules indicated as circles are sheared to positions shown by triangles.

of these low-shear twins would be a useful aid to the understanding of the deformation process.

Stacking faults and twins in the monoclinic phase of polyethylene have not been studied to any great extent, although Crellin [8] has considered the possible twin modes using a two-dimensional, point-lattice analysis, and (010) twinning has been found in transformed regions of single crystals [1]. (For monoclinic indices, the convention employed here is that adopted in Part 1: namely, [001] is the diad axis and the "*a*-direction" of the unit cell (Fig. 1c of [9]) is [100].) There are several modes for twinning on (010), the shear magnitudes depending sensitively on cell angle β (Fig. 1c of [9]). For the theoretical value of $\sim 77°$ (see Table II of [9]), the lowest shear of (0.46) corresponds to the mode with elements

$$K_1: (010); K_2: (100); \eta_1: [100]; \eta_2: [010]. \quad (3)$$

Plane-of-shear sketches for (010) and (100) twinning by this mode are given in Fig. 1b. (An equally low shear is associated with the mode $(010)\,(4\bar{1}0)\,[\bar{1}00]\,[140]$, and the shear for this is lower still for the experimental β of 72.1°. An even lower shear of 0.11 accompanies $(100)\,(120)\,[010]\,[\bar{2}\bar{1}0]$ twinning, but only half the chains are sheared to monoclinic sites.) As in the orthorhombic case, there is no obvious reason for the preference of twinning on one plane, i.e. (010), over its reciprocal, i.e. (100), and a study of twin-boundary properties is called for here also.

Probably the only way at present of gaining detailed information about the molecular configuration and boundary energies of the stacking faults and twins referred to above is by computer simulation, provided the model crystals used offer reasonable approximations to polyethylene. The boundaries of coherent faults and twins are periodic in the interface plane and can, therefore, be modelled with a finite number of molecules. A general simulation suite ("DEVILS") has been described in Part 1 [9], and is used here to study these boundaries. As explained in [9], DEVILS describes a model of rigid, infinite chains, and so the characteristic features examined are those due to intermolecular forces well away from surfaces: the effects of surface folds are not explored. It would be necessary to incorporate these at a later date when intracrystalline behaviour is more fully understood.

The method used is described in Section 2. Results for stacking faults and twins in both phases of polyethylene are presented in Section 3 and discussed in Section 4. As was outlined above, dislocations provide important deformation mechanisms in polyethylene, and in some cases are intimately related to stacking-fault stability. They have also been studied by computer simulation, and the results of this investigation form a separate paper (Part 3).

2. Methods

2.1. Stacking faults

A translational stacking fault is created by the relative translation **f** of two parts of a crystal having the same orientation: the "fault vector", **f**, is usually taken to lie in the planar interface between the two parts, but displacement normal to the fault can occur. The energy of a crystal is raised by the presence of such a fault, and the only faults of real interest are those for which the crystal is in equilbrium without external constraint. Such "stable" faults are best revealed as minima on the three-dimensional surface obtained by plotting the stacking-fault energy per unit area, γ, against **f** for a given fault plane [10]. If minima do not exist on such a γ-surface, except for the points when **f** is a lattice vector, stable faults are not possible for that plane. This is the principle employed by the routines of DEVILS in the present study.

The computations were carried out in two stages. In the first, a γ-surface was generated for a chosen plane by calculating γ for a grid of **f**'s without allowing any additional molecular relaxations or rotations to occur: this "unrelaxed" γ-surface was therefore produced relatively quickly. The fault plane $(hk0)$ was chosen as the xz-plane of the crystalline, and periodic boundary conditions were employed in the x direction to simulate an infinite fault. (Periodicity is ensured in the z direction [001] by the rigid-chain assumption of DEVILS [9].) The x dimension of the inner region was the lattice repeat distance in that direction and the y dimension was the shortest compatible with the interatomic potential range, thereby minimizing the computation time. The general fault vector is

$$\mathbf{f} = \alpha[k\bar{h}0] + \beta[001], \qquad (4)$$

and all possible γ values are found with $0 \leqslant \alpha, \beta \leqslant 1$. In all cases examined, the unrelaxed γ-surface was similar in shape to that obtained when molecular relaxations were permitted, although of course the value of γ was higher. Also, no stable minima were found for values of β other than 0 or $\frac{1}{2}$, as expected from symmetry. The second stage of the computation was concentrated, therefore, on likely stable-fault vectors (with $\beta = 0$ or $\frac{1}{2}$) identified in the first stage.

DEVILS utilizes a combination of steps for this relaxation alternately: they employ either "local" molecular relaxation, in which chains are displaced and rotated to minimize energy according to the conjugate-gradients method, or "rigid-body" relaxation, in which the two halves of the crystal are rigidly displaced with respect to each other to minimize forces across the fault plane. The latter step modified **f** – usually by less than 1% of α – and can add to it a component perpendicular to $(hk0)$. The number of xz planes $(hk0)$ specified in the inner region for the relaxation stage depended on the fault-plane index, and was usually between six and ten for most of the relaxations. For all stable faults, however, this number was doubled for a final relaxation; the resulting change in γ was found to be less than 0.5% in all cases.

The planes investigated were the low-index ones considered good candidates for stable faulting, namely $(100)_0$, $(010)_0$, $(310)_0$ and $(130)_0$ for the orthorhombic phase and $(100)_m$, $(010)_m$, $(110)_m$ and $(1\bar{1}0)_m$ for the monoclinic. (The subscripts 0 and m are used here to denote the two structures.) All the simulations used the set I interatomic potentials described in Part 1 [9].

2.2. Twin boundaries

In conventional theories of twinning [6], parent and twin parts of a deformation-twinned crystal have the same crystal structure and are related by either simple reflection in a plane or rotation of π about an axis. These operations refer in particular to reflection in K_1, rotation of π about the normal to K_1, reflection in the plane normal to η_1 and rotation of π about η_1. In these four relationships, the plane K_2 containing η_2 remains undistorted but rotated by the simple shear in the direction η_1 parallel to the twin plane K_1, which is undistorted and unrotated. (For the equally-feasible reciprocal mode, K_1 and η_1 are interchanged with K_2 and η_2.) The more-general definition of a twin [6] is a region that has undergone a homogeneous deformation such that the product is orientated differently from the parent but has an identical

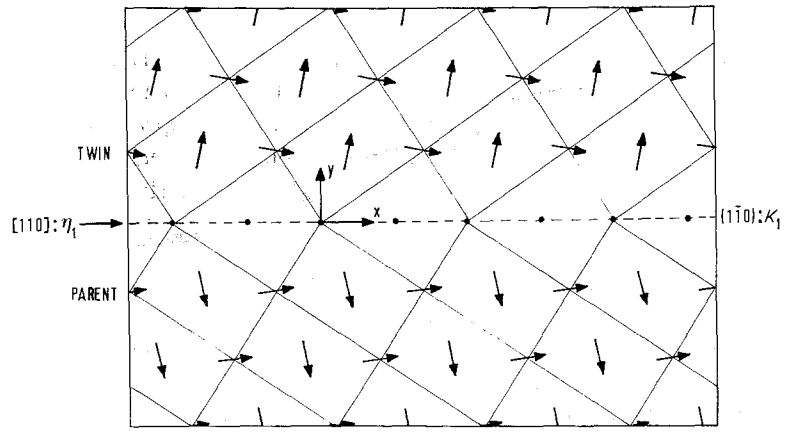

Figure 2 Schematic representation of the conventional simple-reflection twin on $(1\bar{1}0)_o$.

structure; the orientation relationship may be different from reflection or rotation. The twins to be dealt with here are conventional in their orientation but not necessarily in position.

This is demonstrated in Fig. 2, which shows a $(1\bar{1}0)_o$ twin produced in the orthorhombic structure by reflection in K_1, as defined Relation 2: the molecules in the composition plane are shown as points since there are no crystallographic grounds for determining their setting angles. The twin produced by rotation of π about the normal to K_1 is the same as that shown in Fig. 2, whereas the other two conventional twin relationships have chains at the sites shown in Fig. 2 but with the arrows reversed, which is equivalent to the twin in the figure undergoing a rigid translation of $\frac{1}{2}[001]$. These four conventional twins are shown schematically in Fig. 3a and b. Two other twins can be produced from these simply by rigid-body translations of $\frac{1}{2}[001]$ and/or $\frac{1}{2}[110]$, however, as shown in Fig. 3c and d, so that four distinguishable interfaces exist. (There are, similarly, four variants for the $(310)_o$, $(100)_m$ and $(010)_m$ twins also examined here.) In the general case, furthermore, the rigid translations which relate parent and twin need not be restricted to $\frac{1}{2}[001]$ and $\frac{1}{2}\eta_1$. Indeed, from our earlier work on the $(110)_o$ twin in polyethylene [11] and similar theoretical and experimental work in metals [12, 13], it is known that the low-energy, stable boundary is likely to be one corresponding to translation across the interface from the conventional position.

The simulations of coherent twin boundaries, therefore, paralleled the stacking-fault investigation, in that the rigid-body translations of the stable interfaces were sought (in addition to their energy and molecular structure). The $\{110\}_o$, $\{310\}_o$, $(100)_m$ and $(010)_m$ twins were chosen for study on the grounds of probable importance. The routines of DEVILS were first used to create a twinned crystalline with a simple reflection boundary on $(hk0)$, such as that for $(1\bar{1}0)_o$ shown in Fig. 2. The unrelaxed twin-boundary

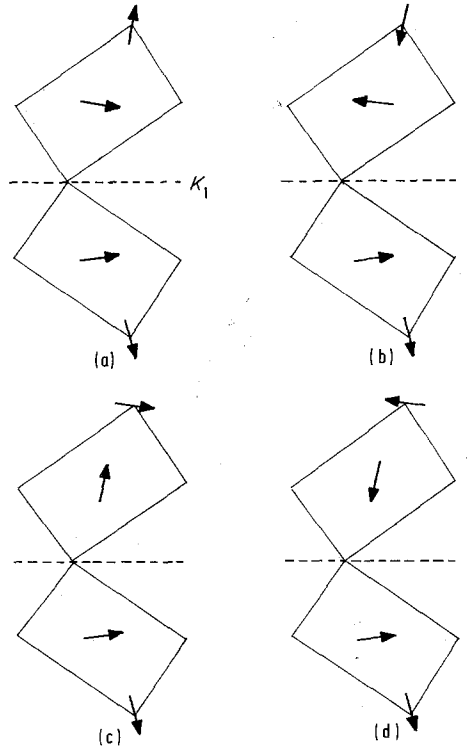

Figure 3 The four conventional $\{110\}_o$ twin relationships. The unit cell is reflected in K_1, but rigid translations in (b), (c) and (d) destroy the reflection symmetry of the molecular units in (a).

energy was computed for a grid of rigid-body translations with vectors of the form

$$\mathbf{t} = \alpha[k\bar{h}0] + \beta[001], \qquad (5)$$

where $0 \leqslant \alpha, \beta \leqslant 1$. (As with stacking faults, stable interfaces with z translations other than $\beta = 0$ or $\frac{1}{2}$ are not expected and were not found in any runs for which they were employed.) Energy minimization of the twinned crystallites was then undertaken allowing both local-molecular relaxations and rigid-body translations, particular attention being paid to regions on the unrelaxed-energy surface identified as possible minima. Economy of mill time was achieved by using small blocks with six $(hk0)$ planes in the inner region for most relaxations and only embedding into a block with twelve planes for a final minimization: this step was found to affect the relaxed twin-boundary energy by less than 0.5% in all cases. Again, all simulations employed the set I interatomic potentials [9].

3. Results

3.1. Stacking faults

Isometric γ-surface plots of the unrelaxed stacking-fault energy γ_u for the $(100)_0$, $(010)_0$ and $(110)_0$ faults in the orthorhombic phase are shown in Fig. 4a to c. Each was generated from a

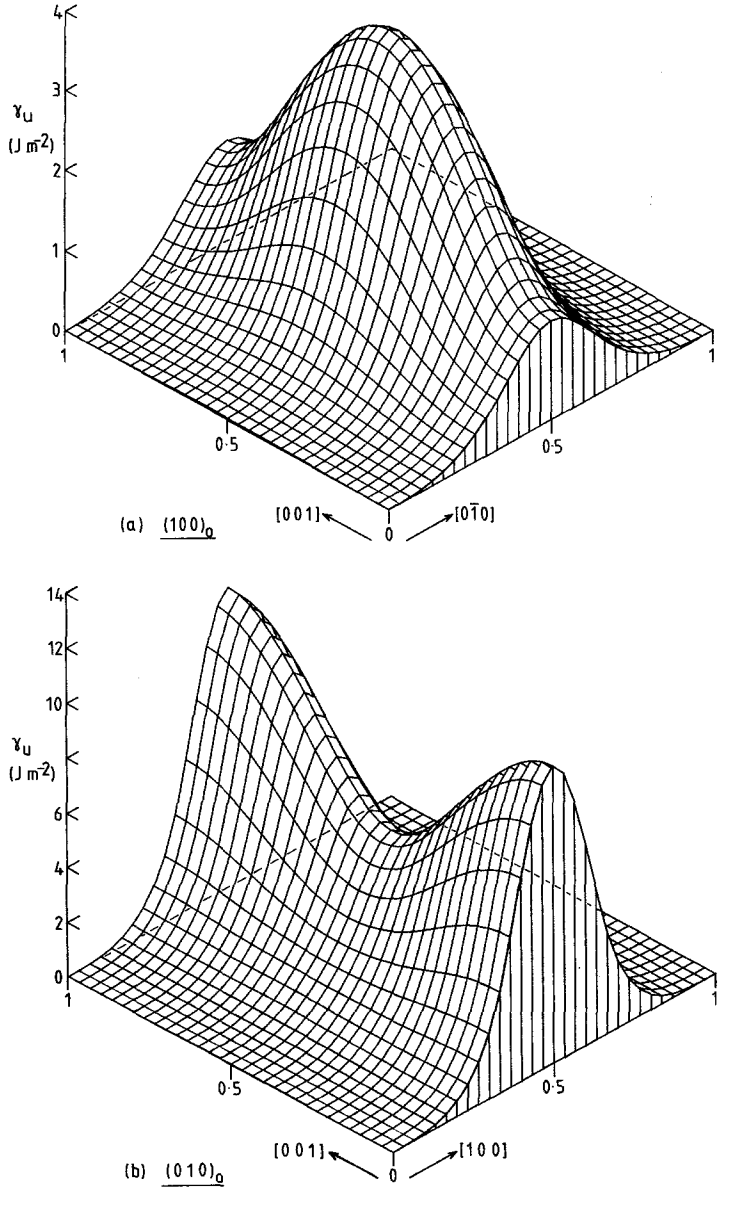

Figure 4 Isometric surface plots of the unrelaxed stacking-fault energy, γ_u, for (a) the $(100)_0$, (b) the $(010)_0$ and (c) the $(110)_0$ planes.

Figure 4 Continued

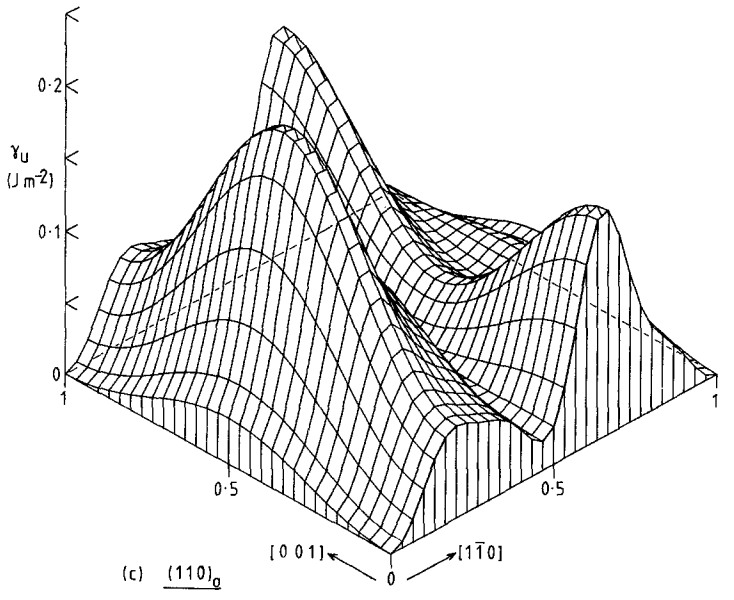

30 × 30 grid of points given by varying α and β in Equation 4. For a given α shift, the variation of γ_u with [001] translation is approximately sinusoidal with period c, consistent with the interaction between combinations of periodic atomic rows and the crystal symmetry. Values of β other than 0 or $\frac{1}{2}$ can, therefore, be neglected. The stable minima at the corners of the γ surfaces, i.e. α and $\beta = 0$ or 1, correspond to perfect crystals, and clearly, therefore, stable stacking faults do not exist on $(100)_0$ and $(010)_0$. The topography of the surface for $(110)_0$, however, reveals the possible existence of one or more stable faults when α is approximately 0.5 and 0.8. This is seen more clearly in Fig. 5a, which shows the variation of γ_u with α for $\beta = 0$ or $\frac{1}{2}$ for the $(110)_0$ plane. Four stable translations appear to be possible, corresponding to (α; β) values of (0.47;0), (0.52; 0.5), (0.77; 0.5) and (0.97; 0.5). (Although the second and last of these are unstable with respect to [001] shifts in the unrelaxed state, they may be stable after relaxation and cannot, therefore, be neglected.) Similar studies of the $(310)_0$ and $(130)_0$ planes indicate the probable presence of faults on these also, as can be seen from the γ_u plots of Fig. 6a and b. The unrelaxed faults listed in Table I were, therefore, selected for simulations involving relaxations.

Local molecular relaxations with the outer, fixed regions of the crystal held at a given **f** vector change the detailed shape of the γ surface but not, in general, its form. The peaks on the surface are reduced typically by factors of 4 or more and the troughs by factors of about 2, and the α values of the minima are close to those obtained from the γ_u curves. This is demonstrated by the plots of relaxed energy, γ_R against α for $(110)_0$ faults in Fig. 5b, for which the forty data points were obtained for crystals containing six (110) planes in the inner region. The final energy minimization for faults identified from such γ_R curves were obtained using larger blocks with alternating molecular and rigid-body relaxations, as explained in Section 2, and the stable-fault vectors and energies are listed in Table II. The vectors are little changed from those in Table I, but in all cases the minimization of energy and interfacial forces required small translations of the outer crystal regions perpendicular to the

TABLE I Unrelaxed stacking faults energies in orthorhombic and monoclinic polyethylene

Fault plane	Shift vector **f**	Unrelaxed boundary energy, γ_u (mJ m^{-2})
$(110)_0$	[0.47, −0.47, 0]	19.7
$(110)_0$	[0.52, −0.52, 0.5]	23.9^{u*}
$(110)_0$	[0.77, −0.77, 0.5]	34.1
$(110)_0$	[−0.03, 0.03, 0.5]	27.8^{u}
$(310)_0$	[0.49, −1.57, 0]	17.6
$(130)_0$	[1.5, −0.5, 0]	30.9
$(130)_0$	[1.5, −0.5, 0.5]	31.6^{u}
$(100)_m$	[0, −0.44, 0.5]	20.1
$(100)_m$	[0, 0.15, 0.5]	4.7
$(010)_m$	[−0.41, 0, 0]	11.4^{u}
$(010)_m$	[−0.18, 0, 0]	6.6

^{*u} denotes unstable equilibrium.

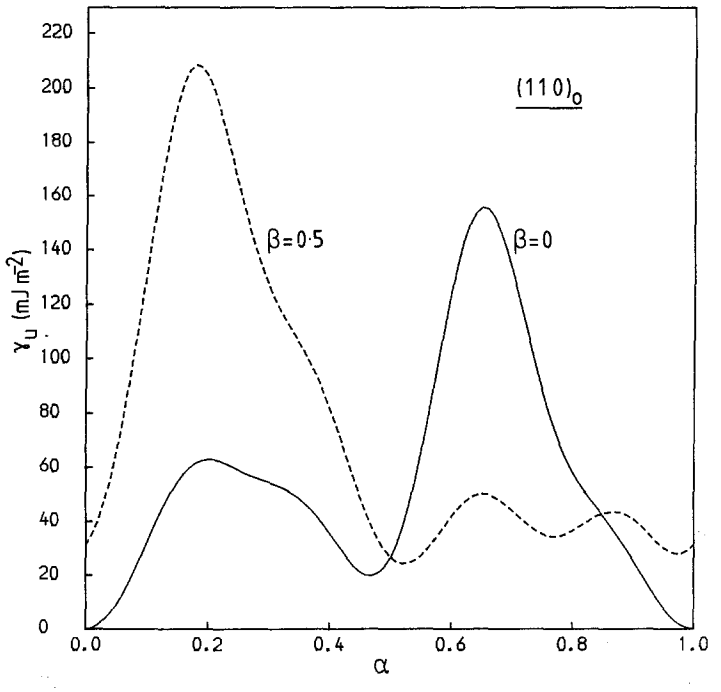

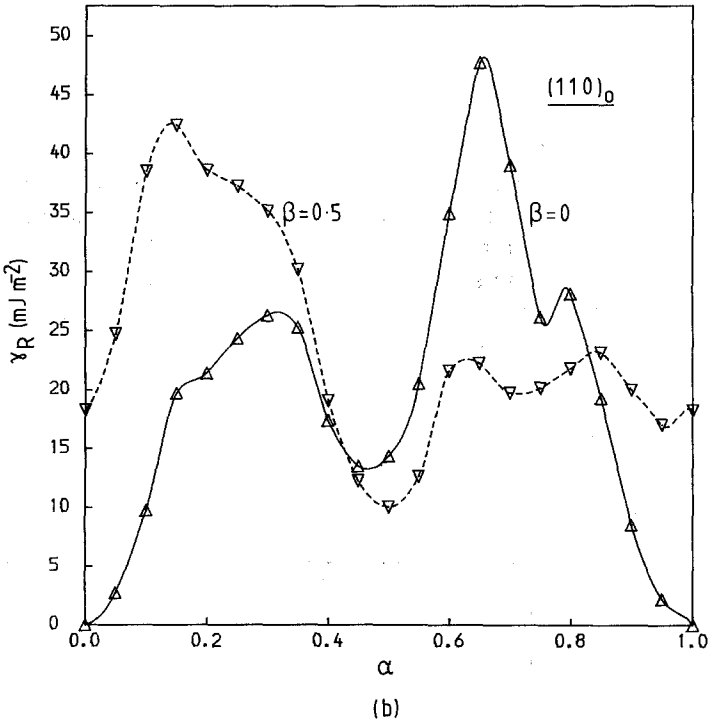

Figure 5 Variation of (a) unrelaxed, γ_u, and (b) partially-relaxed, γ_R, stacking-fault energy with fault vector $\alpha[1\bar{1}0]$ on the $(110)_0$ plane. The values $\beta = 0$ and 0.5 correspond to shifts of zero and $c/2$ in the [001] direction.

fault plane. These volume expansions are included in Table II.

The simulations of monoclinic crystals followed a similar pattern, with the γ_u curves indicating the possible existence of stable faults on $(100)_m$ (see Fig. 7a) and $(010)_m$, but not $(110)_m$ (Fig. 7b) or $(1\bar{1}0)_m$ (Fig. 7c). The $(010)_m$ energy surface (Fig. 8a) shows a translation giving a γ-value of zero: this is because the vectors $\frac{1}{2}[101]$ and $\frac{1}{2}[10\bar{1}]$ are lattice vectors of the structure. The

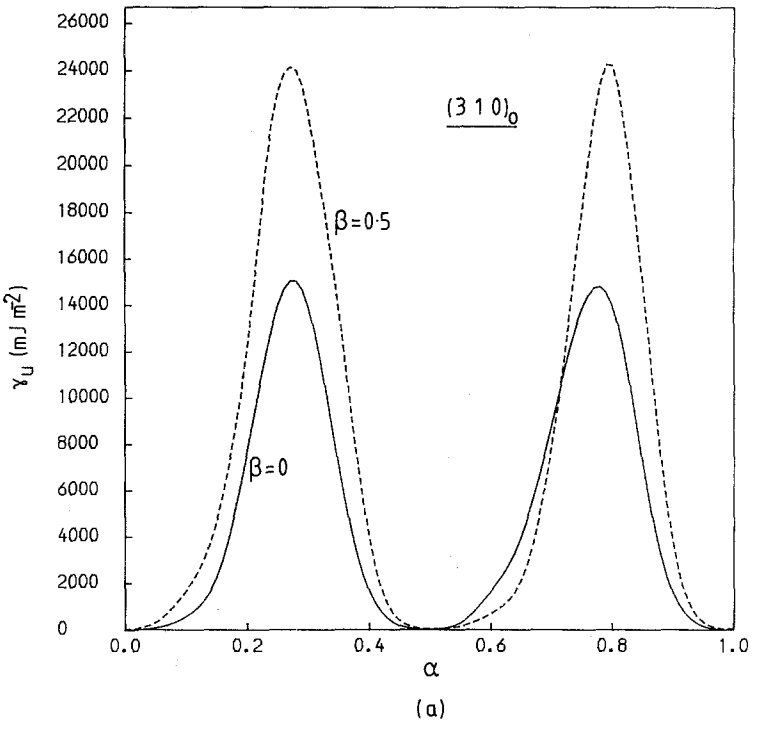

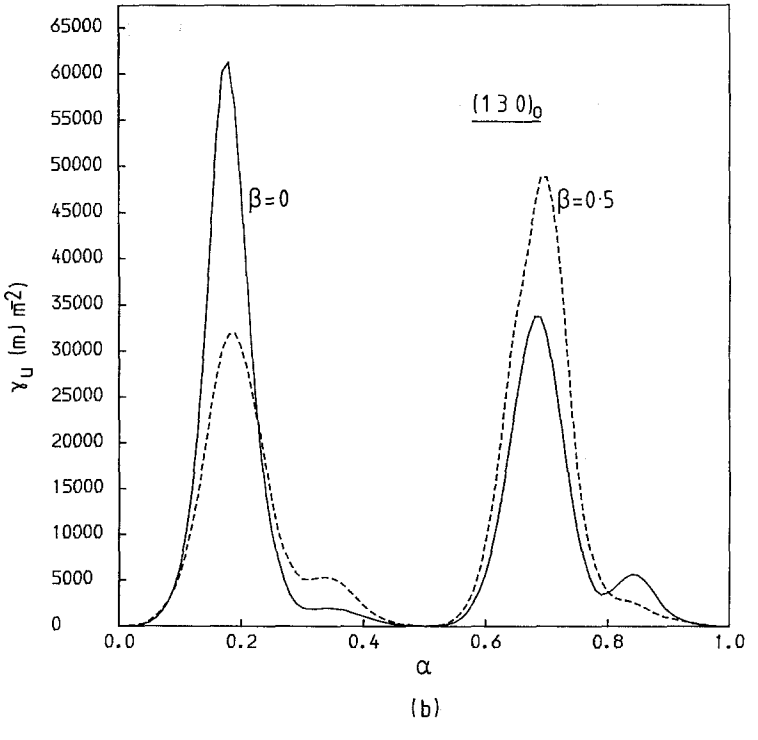

Figure 6 Variation of unrelaxed stacking-fault energy, γ_u, with α for translations of (a) $\alpha[1\bar{3}0]$ on $(3\,1\,0)_0$ and (b) $\alpha[3\bar{1}0]$ on $(1\,3\,0)_0$. The curves labelled $\beta = 0.5$ correspond to additional translation of $\frac{1}{2}[0\,0\,1]$.

faults produced by the translations given in Table I were relaxed partially (see Fig. 8b, for example) and then fully, and the faults listed in Table II were found to be stable. The volume expansion for the $(1\,0\,0)_m$ faults was negligible.

3.2. Twin boundaries

The unrelaxed energy, γ_T, of the coherent boundary for the $(1\,1\,0)_0$ twin as a function of rigid-body translation away from the conventional reflection position is shown by the energy surface

TABLE II Possible stacking faults in orthorhombic and monoclinic polyethylene with fully-relaxed fault energies

Fault plane	Shift vector (after relaxation) **f**	Expansion normal to plane fault	Relaxed boundary energy ($mJ\ m^{-2}$)
$(110)_o$	[0.466, −0.466, 0]	1.4%	12.5
$(110)_o$	[0.516, −0.516, 0.5]	0.3%	10.2
$(110)_o$	[0.743, −0.743, 0.5]	3.7%	17.7
$(310)_o$	[0.497, −1.491, 0]	0.1%	10.2
$(130)_o$	[1.5, −0.5, 0]	5%	17.4
$(130)_o$	[1.5, −0.5, 0.5]	2.8%	9.7
$(100)_m$	[0, −0.45, 0.5]	–	10.4
$(100)_m$	[0, 0.15, 0.5]	–	3.4
$(010)_m$	[−0.415, 0, 0] [0.085, 0, 0.5]	1%	9.5
$(010)_m$	[−0.226, 0, 0] [0.274, 0, 0.5]	1.3%	3.6

of Fig. 9a. This immediately suggests that none of the conventional parent-twin interfaces (Fig. 3) are stable with respect to translation. The same is true for the $(310)_o$, $(100)_m$ and $(010)_m$ twins, as indicated by the unrelaxed-energy curves of Figs. 10a to c, respectively, although some minima are close to $\alpha = 0$. All the (possibly-stable) minima identified from the unrelaxed-energy calculations are listed in Table III. The $(010)_m$ curves reveal the invariance with respect to the $\frac{1}{2}[101]$ lattice translation vector referred to in Section 3.1.

On subsequent partial relaxation with local molecular displacements and rotations allowed, the energies decreased, as shown by the example for the variation of γ_R with α for the $(110)_o$ twin reproduced in Fig. 9b. The energies, translation vectors and volumes for the fully-relaxed orthorhombic and partially-relaxed monoclinic stable boundaries are given in Table IV. (The time-consuming, full relaxations were omitted in the latter cases, but the energies should be within 5% to 10% of the true values.) The $(310)_o$ twins

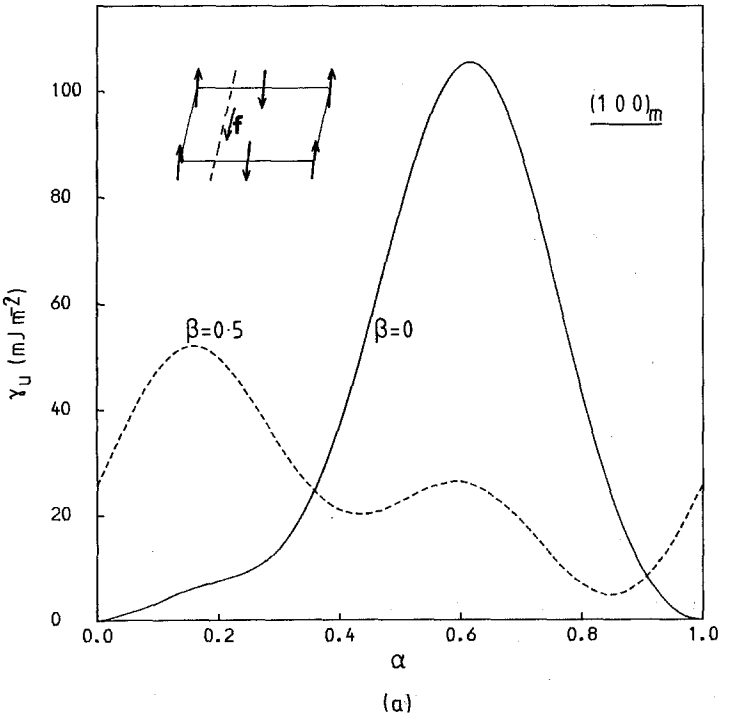

Figure 7 Variation of unrelaxed stacking-fault energy γ_u, with α for translations of (a) $\alpha[0\ \bar{1}\ 0]$ on $(1\ 0\ 0)_m$, (b) $\alpha[1\ \bar{1}\ 0]$ on $(1\ 1\ 0)_m$, and (c) $\alpha[\bar{1}\ \bar{1}\ 0]$ on $(1\ \bar{1}\ 0)_m$. The curves $\beta = 0.5$ correspond to additional translation of $\frac{1}{2}[0\ 0\ 1]$.

Figure 7 Continued

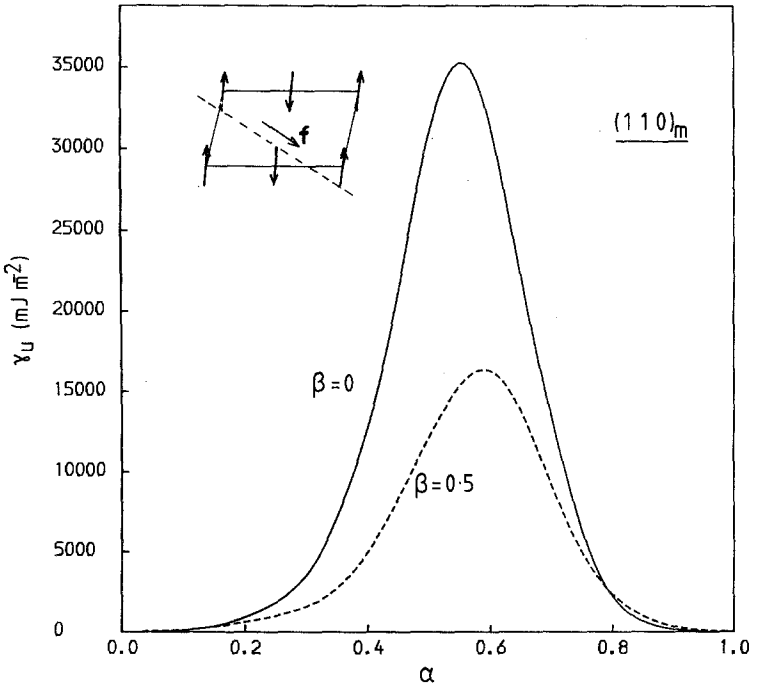

(b)

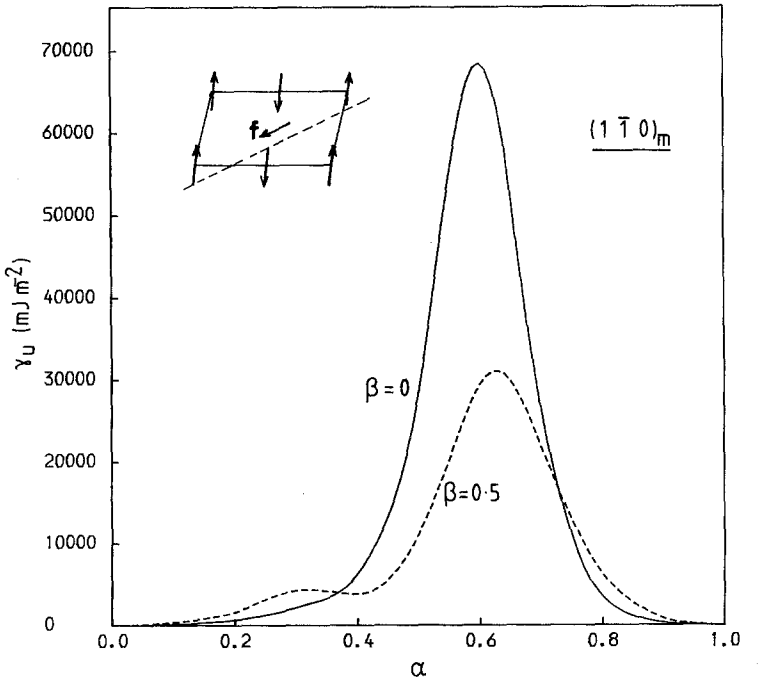

(c)

have much higher boundary energy than the $(1\,1\,0)_0$ twins, and their associated volume expansions are correspondingly greater. Similarly, the $(0\,1\,0)_m$ twins have lower energy than the $(1\,0\,0)_m$ twin interfaces.

4. Discussion

4.1. Boundary stability

The stability of all the boundary configurations reported in the preceding section has been checked by imposing rigid shifts of 0.1 [001] on the

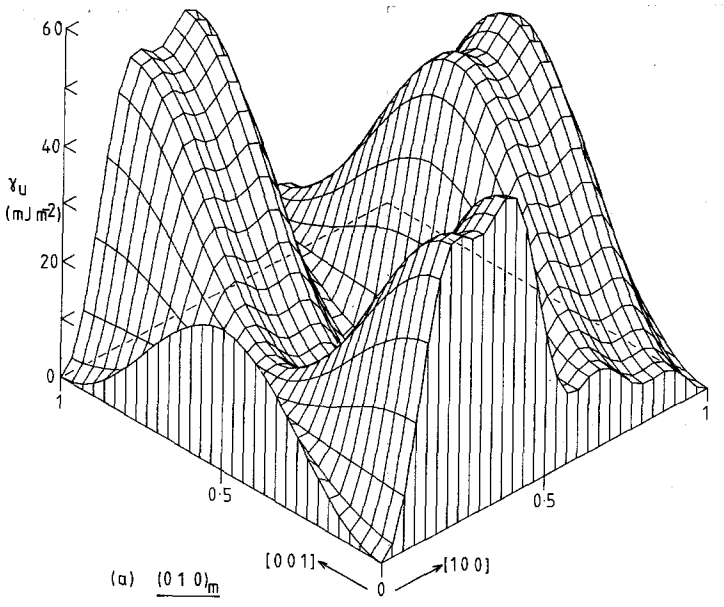

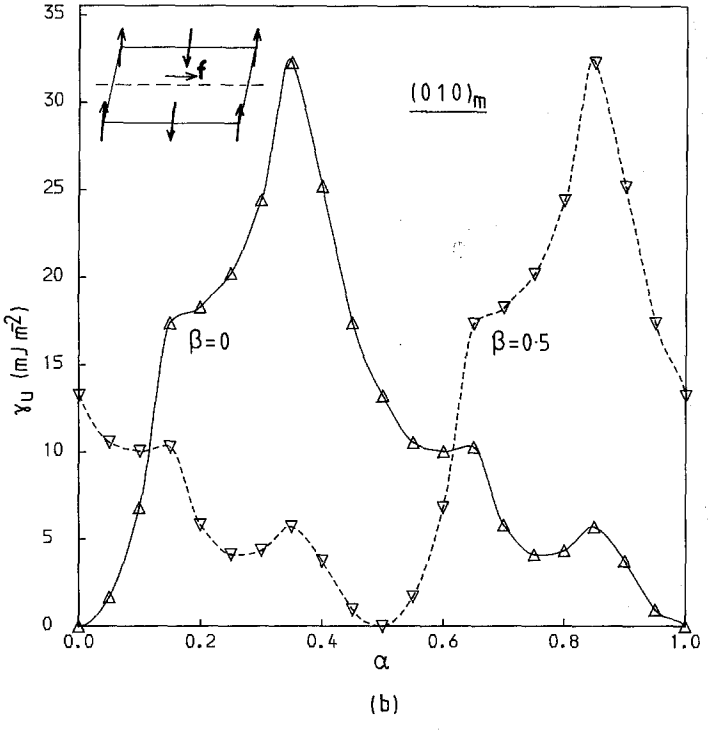

Figure 8 (a) Isometric surface plot of the unrelaxed stacking-fault energy, γ_u, on the $(010)_m$ plane. (b) Variation of partially-relaxed fault energy, γ_R, with fault vector $\alpha[100]$ on the $(010)_m$ plane for shifts of zero and $c/2$ in the [001] direction.

translations listed, and then allowing further relaxations: the original structure was always recovered. It should be emphasized that the stacking-fault and coherent-twin energies quoted refer to crystals in equilibrium under the set I non-bonded interatomic potentials described in Part I [9]. Such energies can be rather sensitive to the shape and range of interatomic potential, and should be considered as data for a model crystal rather than physical parameters for polyethylene. In order to examine this point further, unrelaxed γ-surfaces for stacking faults were generated for $(100)_0$, $(010)_0$ and $(110)_0$ using the set VII and set VIII (Truncated) potentials [9]. The latter set is markedly different from set I in that the ranges are small. The overall form of the γ-surface was found to be very similar to that for set I in each case. The vectors of the

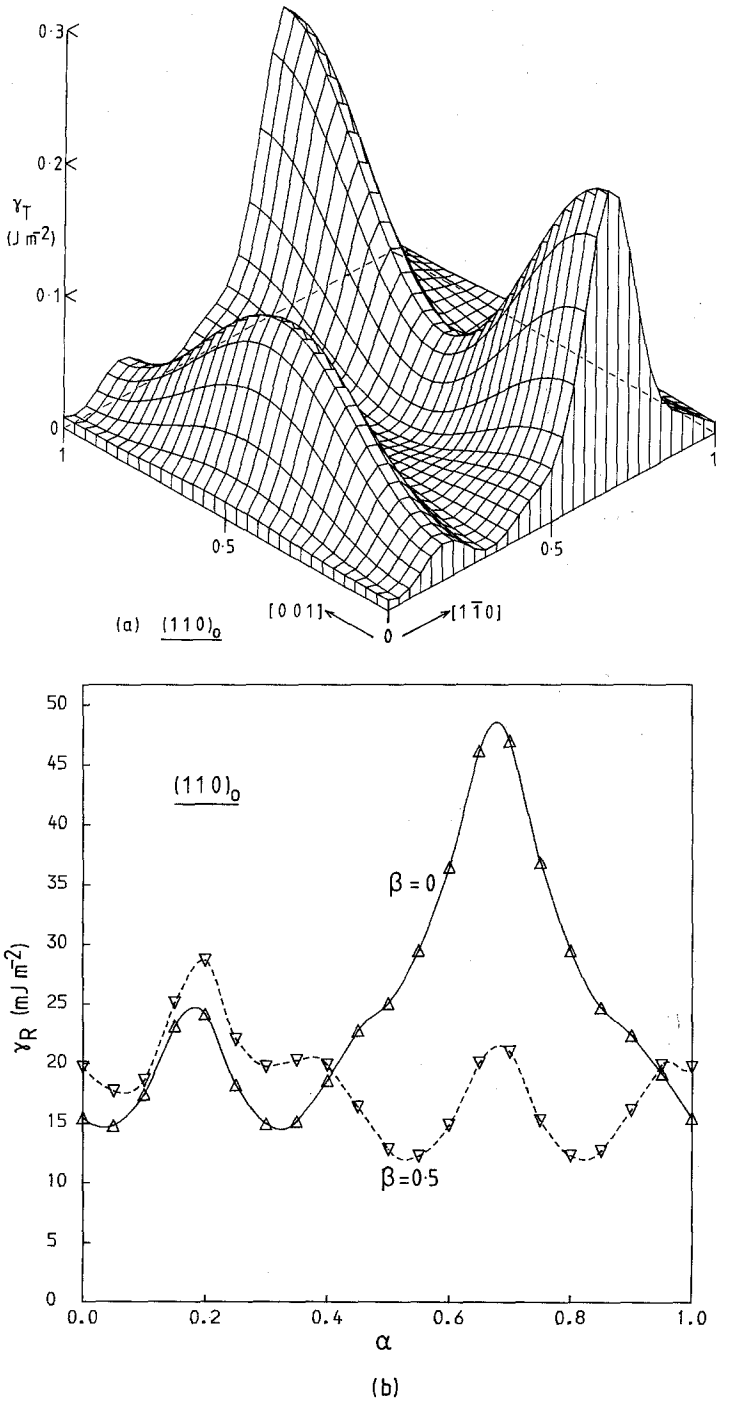

Figure 9 (a) Isometric surface plot of the unrelaxed boundary energy, γ_T, for the $(1\,1\,0)_0$ twin. (b) Variation of the partially-relaxed boundary energy with translation $\alpha[1\bar{1}0]$ for the $(1\,1\,0)_0$ twin: $\beta = 0.5$ refers to an additional translation of $\frac{1}{2}[001]$.

stable $(1\,1\,0)_0$ faults were in close agreement, the $(\alpha; \beta)$ values for the minima with respect to the $[1\bar{1}0]$, [001] translations being (0.47; 0), (0.53; 0.5) and (0.81; 0.5) for both set VII and set VII (Truncated); the corresponding γ_u energies are 25.9, 33.6 and 45.9 mJ m^{-2}, respectively, for set VII, and 22.0, 24.4 and 38.5 mJ m^{-2}, respectively, for set VII (Truncated). Comparison with Table I shows that the fault vectors are little changed; and, in fact, all the translations found here are believed to be realistic, for, as discussed below, they can be demonstrated to have features that are not potential-dependent. The dependence of γ on potential range is small and probably reflects the fact that the faults involve nearest-neighbour changes. The energies obtained suggest that the

relative energy values given in Section 3 have significance and they should provide at least a good guide to the energies one may expect for polyethylene.

The presence of stable faults for shift parameter $\alpha \simeq 0.5$ on $\{110\}_0$ and $\{130\}_0$ of the orthorhombic phase suggests that low-energy faults may also exist on $\{150\}_0$, $\{170\}_0$, etc.,

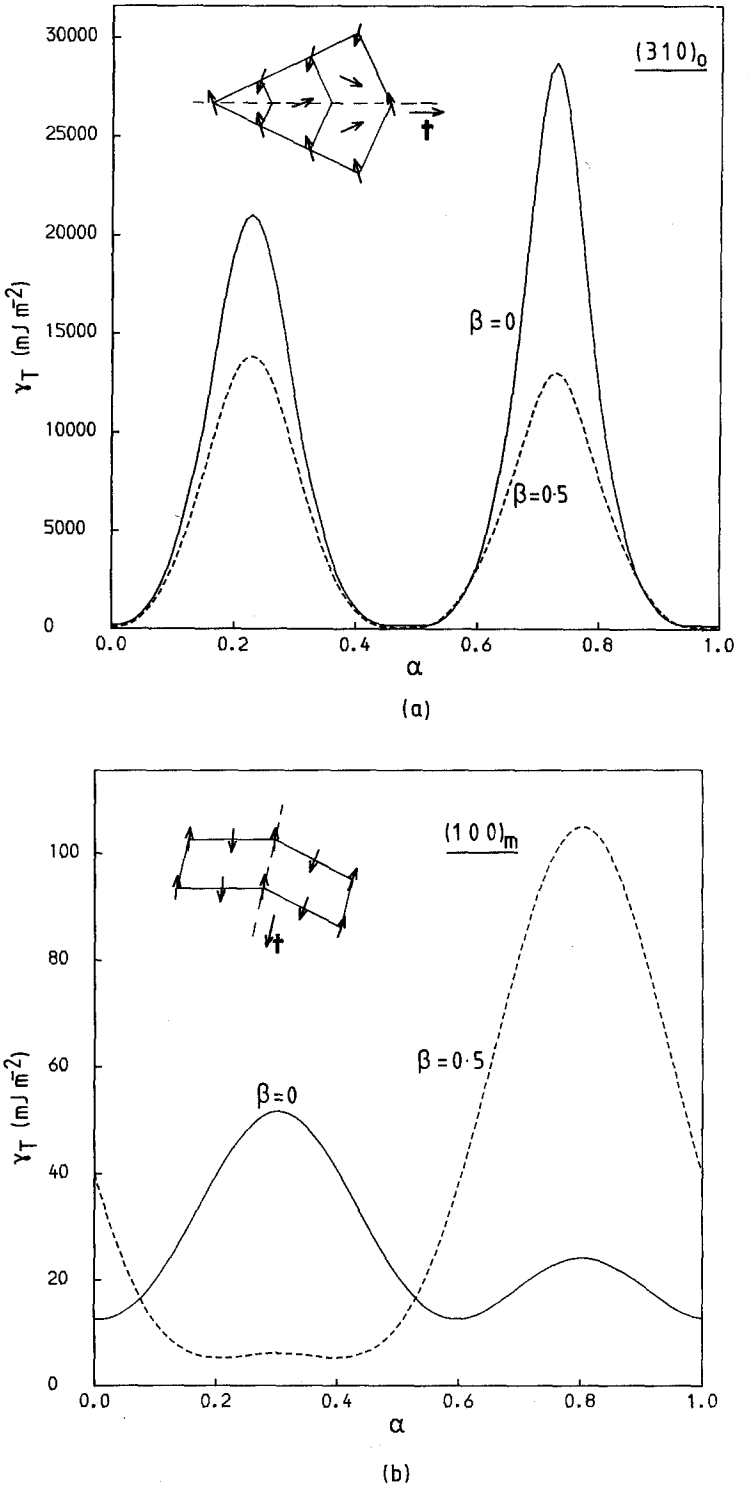

Figure 10 Variation of unrelaxed twin-boundary energy, γ_T with α for translations of (a) $\alpha[1\bar{3}0]$ on $(310)_0$, (b) $\alpha[0\bar{1}0]$ on $(100)_m$, and (c) $\alpha[100]$ on $(010)_m$. The curves $\beta = 0.5$ are for additional translation of $\frac{1}{2}[001]$.

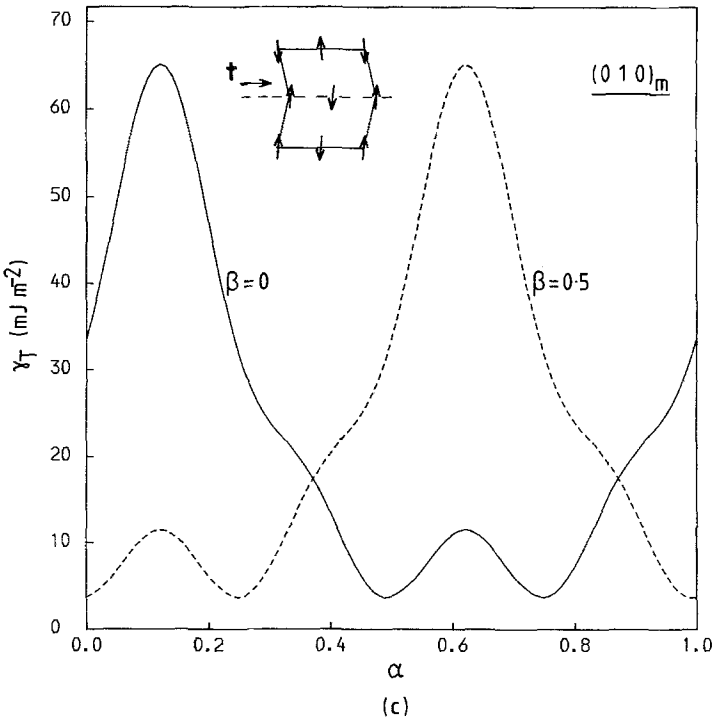

Figure 10 Continued

for similar values of α. The γ_u form of the $(5\,1\,0)_0$ plane was therefore investigated and a stable fault of $\gamma_u = 14.8\,\mathrm{mJ\,m^{-2}}$ at $\alpha = 0.5$ revealed. Whilst this energy is even lower than that on $(1\,1\,0)_0$, the $\frac{1}{2}[1\bar{5}0]$ vector required to create it is too large for any conceivable dislocation mechanism, and the energy barrier to be overcome in achieving such faults increases rapidly with increasing index. They have not, therefore, been considered further. It is possible that stable faults exist on other planes, and, indeed, faults are seen on the γ_u curves for $(1\,2\,0)_0$ and $(2\,1\,0)_0$. Their energies are several orders of magnitude higher ($\sim 5\,\mathrm{J\,m^{-2}}$) than the $\{1\,1\,0\}$ faults, however, and were not examined in detail. The faults listed in Table II are considered to be the only ones of significance.*

The molecular structures of the $(1\,1\,0)_0$ stacking fault with $\mathbf{f} = [0.52, -0.52, 0.5]$ and the three $(1\,1\,0)_0$ twins with $\mathbf{t} = [0.04, -0.04, 0]$, $[0.32, -0.32, 0]$ and $[0.83, -0.83, 0.5]$ are shown in Fig. 11. (The twin structure in Fig. 11d and the γ against α curves of Figs. 6 and 8, are very close to the results of our previous simulation of $\{1\,1\,0\}_0$ twins [12]: the minimum γ_R is higher, however, owing to an error in a numerical parameter employed earlier.) The stability of these and the other structures, and also the general form of the γ surfaces and curves presented in Section 3, can be understood by consideration of the interaction of the molecules that are nearest neighbours across the interface plane. As the **f** and **t** translations are undertaken from the perfect-crystal and conventional-reflection-twin states, respectively, peaks on the energy surface arise when the molecules are at positions of closest approach. The peaks are higher for high-index planes and are particularly large when the setting angles are such that the hydrogen–hydrogen separation is small. The energy minima, on the other hand, always correspond to situations where adjacent pairs of nearest-neighbour chains form interfacial polygons which approximate to parallelograms with acute angles between 70° and 80°. These shapes are denoted by dashed lines in Fig. 11, the angles being 79° for (a) and 73° for (b), (c) and (d), and are characteristic features of all the stacking-fault and twin boundaries found in both crystal structures. As examples, those which form the boundary repeat units for the lowest-energy stacking faults on $(3\,1\,0)_0$, $(1\,3\,0)_0$, $(1\,0\,0)_m$, $(0\,1\,0)_m$ and twins on $(3\,1\,0)_0$, $(1\,0\,0)_m$, $(0\,1\,0)_m$ are shown schematically in Fig. 12a to g, respectively.

*The $(1\,0\,0)_0$ fault considered by Wunderlich [14] is not a true, translational fault, for it requires the insertion of a complete (1 0 0) plane of molecules, and might occur, for example, in growth.

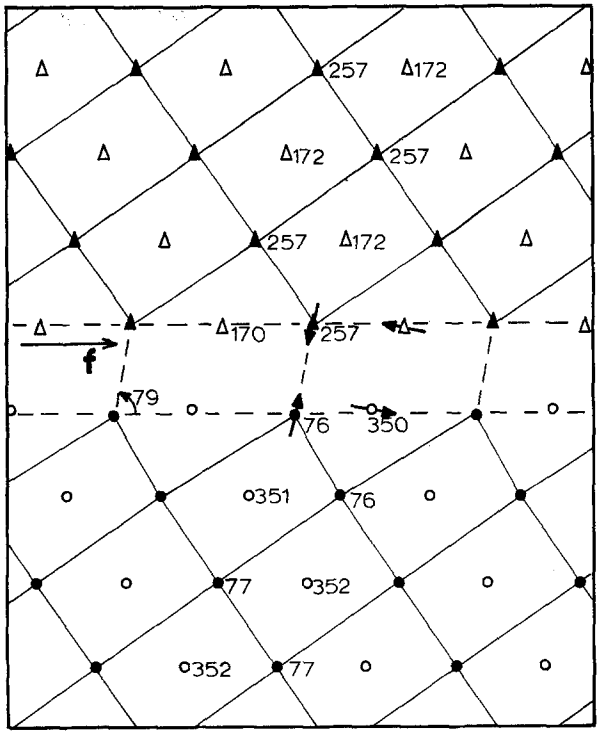

(a)

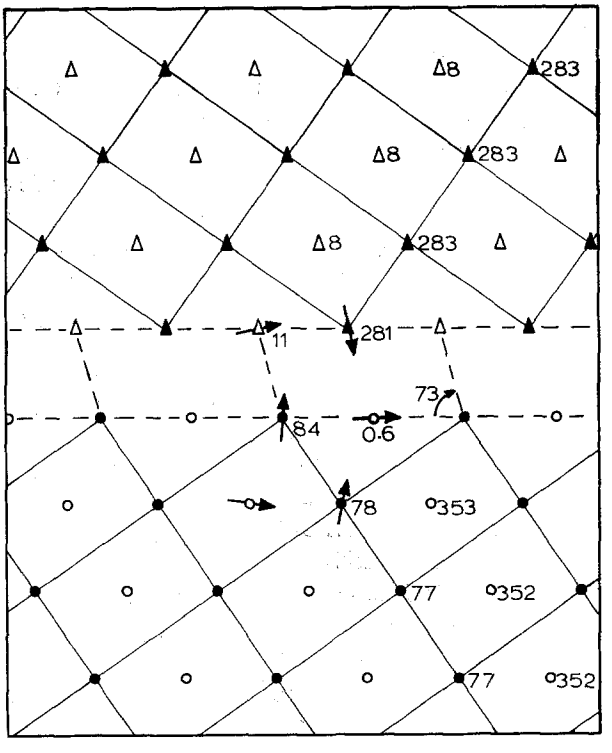

(b)

Figure 11 (a) The boundary structure of the stable $(1\,1\,0)_0$ stacking fault with vector $\mathbf{f} = [0.516, -0.516, 0.5]$ and energy $10.2\,\mathrm{mJ\,m^{-2}}$. Structures for the stable $(1\,1\,0)_0$ twin boundaries with $\mathbf{t} = [0.041, -0.041, 0]$, $[0.316, -0.316, 0]$ and $[0.826, -0.826, 0.5]$ are given in (b), (c) and (d) respectively. Circles represent chain sites in the parent crystal and triangles those in the product: the filled triangles were originally at filled circle sites in (a) and were at the reflection sites of filled circles before translation in (b), (c) and (d). For clarity, the chain orientation vectors are shown only for chains near the interface; numbers next to chains are the setting angles (in degrees) measured from $[1\bar{1}0]$.

Figure 11 Continued.

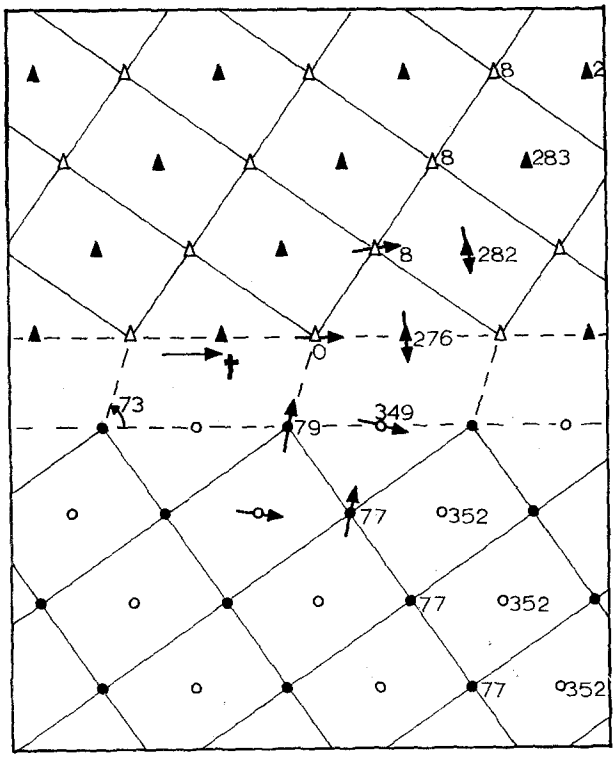

(c)

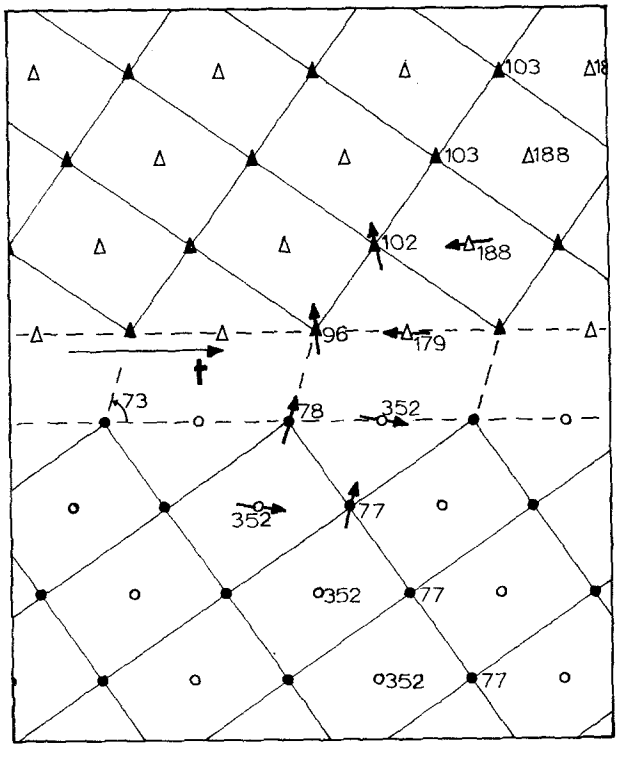

(d)

TABLE III Local minima in the unrelaxed twin boundary energy for various rigid shifts, **t**, in orthorhombic and monoclinic polyethylene

Twin plane, K_1	Shift vector, **t**	Unrelaxed boundary energy, γ_T (mJ m^{-2})
$(110)_o$	[0.04, −0.04, 0]	27.8
$(110)_o$	[0.31, −0.31, 0]	27.8
$(110)_o$	[0.5, −0.5, 0.5]	23.1
$(110)_o$	[0.85, −0.85, 0.5]	23.1
$(310)_o$	[−0.03, 0.09, 0]	162.5
$(310)_o$	[0.49, −1.47, 0]	162.5
$(310)_o$	[−0.02, 0.06, 0.5]	58.5
$(310)_o$	[0.48, −1.44, 0.5]	58.5
$(100)_m$	[0, −0.01, 0]	12.7
$(100)_m$	[0, −0.6, 0]	12.7
$(100)_m$	[0, −0.21, 0.5]	5.3
$(100)_m$	[0, −0.39, 0.5]	5.3
$(010)_m$	[0.49, 0, 0]	3.6
$(010)_m$	[0.75, 0, 0]	3.6
$(010)_m$	[0.25, 0, 0.5]	3.6
$(010)_m$	[−0.01, 0, 0.5]	3.6

These structures can be explained by the fact that stability occurs when the neighbour-to-neighbour lines across the interface complete coordinations that approximate to the perfect crystal. The latter are shown in Fig.13 (with dimensions for the set I potentials), from which it can be seen that the interfacial polygons combine small distortions of these units with chain rotations through approximately 90° or 180°. It is probable that any potentials that describe perfect crystals in equilibrium will produce similar boundary structures, and the geometries found, therefore, are of general validity. From the molecular geometry of the boundaries in Fig. 11b and c, it is easy to see why their energies are the same: the other twin energies are paired for the same reason.

4.2. Stacking faults and slip

The shape of the γ surface for a particular plane is related to the core structure and ease of movement of dislocations on that plane [10], for it is determined by the geometry and form of the intermolecular forces spanning the plane. In particular, the total restoring force $\mathbf{F}(= -\text{grad}\ \gamma)$ divided by the shear modulus appropriate to the direction of translation determines the "width" of the core of dislocations with Burgers vectors in that direction. A maximum in **F** corresponds to a narrow width and a minimum to a wider region of core for a given vector. Furthermore, a fault displacement **f** defining a stable minimum in γ corresponds to the Burgers vector **b** of a partial dislocation bounding a stable fault. The computer models for orthorhombic crystals have shown that faults do not exist on $(100)_o$ and $(010)_o$, but point to complex possibilities on $(110)_o$. The $(110)_o$ fault vectors of Table II are shown schematically in Fig. 14a as ***AL***, ***AM*** and ***AN*** and imply the existence of partial Burgers vectors of the form ± ***AL, AM, AN, LB, LC, LD, LM, LN, MD, MN, ND***, together with any of these added to ± [001], etc.

As far as orthorhombic, chain-axis slip with

TABLE IV Stable relaxed twin boundaries in orthorhombic and monoclinic polyethylene

Twin plane, K_1	Shift vector, **t**	Expansion normal to K_1	Relaxed boundary energy (mJ m^{-2})
$(110)_o$	[0.041, −0.041, 0]	3%	13.7
$(110)_o$	[0.316, −0.316, 0]	1.6%	13.8
$(110)_o$	[0.503, −0.503, 0.5]	2%	12.0
$(110)_o$	[0.826, −0.826, 0.5]	1.3%	11.5
$(310)_o$	[−0.027, 0.081, 0]	15.2%	50.6
$(310)_o$	[0.487, −1.461, 0]	13.7%	51.9
$(310)_o$	[−0.020, 0.060, 0.5]	8%	32.4
$(310)_o$	[0.480, −1.440, 0.5]	5.3%	33.4
$(100)_m$	[0, −0.01, 0]	*	5.9
$(100)_m$	[0, −0.6, 0]	*	6.0
$(100)_m$	[0, −0.21, 0.5]	*	4.6
$(100)_m$	[0, −0.39, 0.5]	*	4.6
$(010)_m$	[0.49, 0, 0]	*	2.2
$(010)_m$	[0.75, 0, 0]	*	2.3
$(010)_m$	[0.25, 0, 0.5]	*	2.3
$(010)_m$	[−0.01, 0, 0.5]	*	2.2

*Not calculated.

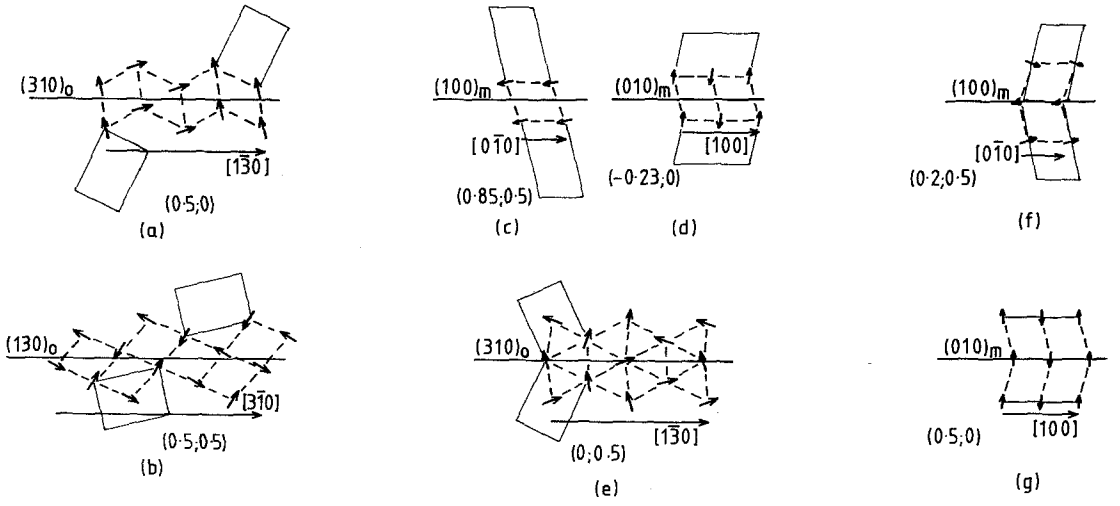

Figure 12 Schematic representation of boundary structures of (a) $(310)_o$, (b) $(130)_o$, (c) $(100)_m$ and (d) $(010)_m$ stacking faults, and (e) $(310)_o$, (f) $(100)_m$ and (g) $(010)_m$ twins. The translation parameters are denoted thus $(\alpha;\beta)$, and the unit cell orientations are shown by faint lines.

$\mathbf{b} = [001]$ is concerned, therefore, dissociation should not occur: even in the least unfavourable case of $DC \rightarrow DM + MC$ on $(110)_o$, Frank's rule shows that dissociation is not possible. From this conclusion and the observation that γ varies approximately sinusoidally when $\mathbf{f}$ lies along [001], it can be surmised that chain-axis slip is most favoured on the plane of the [001] zone with smallest quotient of maximum $\mathbf{F}$ (i.e. smallest maximum γ) divided by the appropriate shear modulus. Of the planes considered here, $(100)_o$, $(010)_o$ and $(110)_o$ have the lowest maximum γ (at $\mathbf{f} = \frac{1}{2}[001]$), in the ratio 1:1.6:1.3, and from [9] their [100] shear moduli are in the ratio 1:1.8:1.6. There is, therefore, no firm indication that the core width will be greater (and the Peierls stress lower) on one plane rather than the others: a full molecular simulation of the dislocation core is required to shed light on that point. The situation for transverse slip with $\mathbf{b}$ perpendicular to [001] is somewhat different. Dislocations on the low-index systems $(100)_o$ [010] and $(010)_o$ [100] are not expected to dissociate. Comparison of the γ surfaces in Fig. 4a and b suggests that the former system should have the lower Peierls stress, but even that should be much higher than that for [001] slip on the same plane. Dislocations on $(110)_o$ can dissociate, however, the reactions most favoured by Frank's rule being (see Fig. 14a)

$$[1\,\bar{1}\,0] \rightarrow [0.47, -0.47, 0] + [0.53, -0.53, 0], \quad (6)$$

followed by

$$[1\,\bar{1}\,0] \rightarrow [0.52, -0.52, 0.5] + [0.48, -0.48, -0.5] \quad (7)$$

Even though the former involves a fault of higher energy than the latter (see Table II), the reduction in dislocation energy probably more than offsets it. (A full anisotropic-elastic calculation similar to those of Shadrake and Guiu [15] would be required to confirm this.) Both partial vectors bounding the fault in Reaction 6 are shorter in magnitude than [100] and [010], and the maximum value of $\mathbf{F}$ on the γ surface along $[1\,\bar{1}\,0]$ on $(110)_o$ is small in comparison with the values for the $(010)_o$ [100] and $(100)_o$ [010] systems. These factors point strongly to transverse slip being dominated by dislocation glide on $\{110\}_o$. The faults reported in Section 3.2. for other planes of the [001] zone are unlikely to

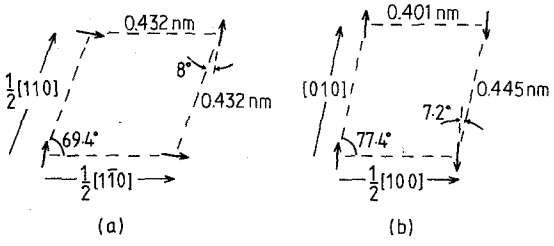

Figure 13 The basic stable units of four molecules for (a) orthorhombic and (b) monoclinic crystals. (The dimensions and angles are for the set I potentials.)

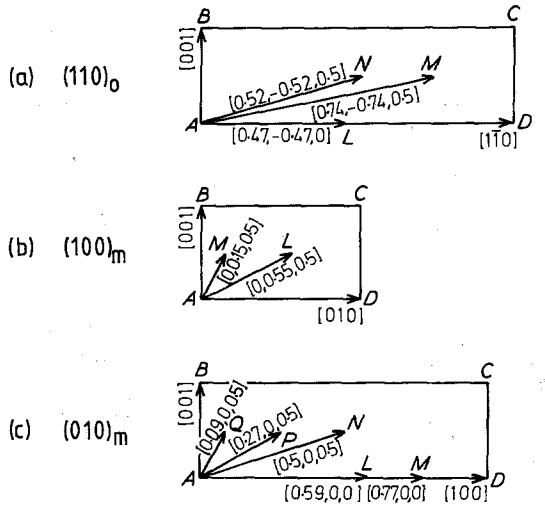

Figure 14 The stable-fault vectors for stacking faults on (a) the $(110)_0$, (b) the $(100)_m$ and (c) the $(010)_m$ planes. The lengths are approximately to scale.

contribute to slip in view of the long Burgers vectors and narrow cores (produced by high **F** values) the partials can be expected to have.

The stable-fault translations found for the monoclinic case are shown schematically for $(100)_m$ and $(010)_m$ in Fig. 14b and c, respectively. As on $(110)_0$, a large number of partial Burgers vectors are possible, although it should be noted that on $(010)_m$ the translations of the form AN generate a perfect crystal, so that Q and P are equivalent to L and M, respectively. The faults at M on $(100)_m$ and M and P on $(010)_m$ have much lower energy than the others (see Table II). The absence of stable faults on $(110)_m$ and $(1\bar{1}0)_m$ suggests that chain-axis [001] slip in the monoclinic phase will occur on $(100)_m$ and $(010)_m$, for dissociations of the form $AB \rightarrow AM + MB$ on $(100)_m$ and $AB \rightarrow AQ + QB$ on $(010)_m$ are possible with an attendant reduction in dislocation energy of about one third, as calculated from the change in $|\mathbf{b}|^2$. Of these two, slip on $(100)_m$ is favoured, for the fault energy is much lower and the width of the partial cores (as measured by $\mathbf{F} = -\text{grad}\,\gamma$) is greater. Transverse slip may also be expected to take place most readily on the two planes that can be faulted. Of the possibilities on the $(100)_m$ [010] system, the dissociation of AD into $AM + ML + LD$ involves the largest reduction in dislocation energy, estimated to be approximately 45% from the change in $|\mathbf{b}|^2$, followed by $AL + LD$ with a reduction of about 30% and $AM + MD$ with a decrease of 10%. The last of these solely involves the low-energy fault, however, and it is not possible to predict which of these dissociations should be dominant with the simple criteria used here. Of the possibilities on $(010)_m$, on the other hand, $\frac{1}{2}[101]$ slip should dominate, for not only is this lattice-translation vector much shorter than [100], but it can dissociate to the low-energy fault by the reaction $AN \rightarrow AP + PN$, with a reduction of 44% in $|\mathbf{b}|^2$. From the shape of the γ surface (Fig. 8a), the two partial cores for this reaction should be relatively wide, and even when the applied stress acts exactly along [100], $(010)_m$ [100] slip can occur by reactions of this type. One would expect, therefore, that $(010)_m$ would be the preferred plane for transverse slip in monoclinic polyethylene.

4.3. General discussion

The geometries of the stable, coherent, twin interfaces are more complicated than previously suspected. The four $(110)_0$ boundaries, in particular, have very similar energies, and a preference for any one over the others cannot be made on the basis of computer models. On energy grounds, the $(110)_0$ twins are favoured over the $(310)_0$, despite their reciprocal relationship, and similarly $(010)_m$ twin boundaries are preferred to $(100)_m$: these conclusions are consistent with the experimental observations discussed in Section 1. They only provide a partial explanation, however, for twinning is a shear mechanism involving the motion of twinning partial dislocations along the interface, and a full study of their structure and properties is required for a complete picture to emerge. This is particularly true in the orthorhombic cases, for the simple shears of low magnitude do not, on their own, restore chains in the twin with the correct setting angles from one plane to the next. It would be possible to incorporate twinning dislocation into the computer models of boundaries studied here, and it is planned that this will be accomplished in the future. For the moment, it is clear from the high restoring forces on the energy surface of the $(310)_0$ twin interface that the twinning dislocations for this mode will have narrow cores and may be relatively difficult to move. Furthermore, the variety of stable structures for all the interfaces suggests that the incoherent boundary associated with twinning dislocations may be complicated by dissociation, as found, for example,

in bcc metals by Bristowe and Crocker [16]. Finally, it should be remarked that the method of computer simulation could be used to investigate the orthorhombic–monoclinic transformation, for both structures are stable with the potentials employed. This stress-induced, martensitic transformation is an important deformation mechanism of polyethylene, and, like twinning, can occur due to a variety of shear modes [1]. (For this reason, the transformation path considered by Yemni and McCullough [17] is not appropriate to this problem.) We hope to report on the nature of the interface and the molecular structure of the transformation dislocations at a later date.

Acknowledgements

The authors thank Professor M. Bevis for drawing their attention to the problem of twin structure in polyethylene and for useful discussions, and acknowledge the SRC for the award of a research studentship to N. A. G.

References

1. M. BEVIS and P. S. ALLAN, *Surface and Defect Properties of Solids* **3** (1974) 93.
2. P. B. BOWDEN and R. J. YOUNG, *J. Mater. Sci.* **9** (1974) 2034.
3. R. J. YOUNG, in "Developments in Polymer Fracture - 1", edited by E. H. Andrews (Applied Science London, 1979) Ch. 7.
4. F. C. FRANK, A. KELLER and A. O'CONNOR, *Phil. Mag.* **3** (1958) 64.
5. V. F. HOLLAND, *J. Appl. Phys.* **35** (1964) 3235.
6. M. BEVIS and E. B. CRELLIN, *Polymer* **12** (1971) 666.
7. J. E. PREEDY and E. J. WHEELER, *J. Mater. Sci.* **12** (1977) 810.
8. E. B. CRELLIN, Ph.D. Thesis, University of Liverpool (1972).
9. D. J. BACON and N. A. GEARY, *J. Mater. Sci.* **18** (1983) 853.
10. V. VITEK, *Crystal Lattice Defects* **5** (1974) 1.
11. N. A. GEARY and D. J. BACON, *Nuclear Metall.* **20** (1976) 479.
12. V. VITEK, A. P. SUTTON, D. A. SMITH and R. C. POND, in "Grain Boundary Structure and Kinetics" (American Society for Metals, Ohio, 1980) p. 115.
13. R. C. POND, *ibid.* p.13.
14. B. WUNDERLICH, "Macromolecular Physics, Vol. I, Crystal Structure, Morphology, Defects" (Academic Press, New York, 1973).
15. L. G. SHADRAKE and F. GUIU, *Phil. Mag.* **34** (1976) 565.
16. P. D. BRISTOWE and A. G. CROCKER, *Acta Metall.* **25** (1977) 1363.
17. T. YEMNI and R. L. McCULLOUGH, *J. Polymer Sci. Polymer Phys.* **11** (1973) 1385.

Received 18 May
and accepted 29 July 1982